C. R. Chimie 18 (2015) 1094–1105

Contents lists available at ScienceDirect

Comptes Rendus Chimie

www.sciencedirect.com

International Symposium on Air & Water Pollution Abatement Catalysis (AWPAC) – Catalytic pollution control for stationary and mobile sources

Combustion synthesis and properties of nanocrystalline zirconium oxide

Izabela Dobrosz-Gómez [a,*], Miguel Ángel Gómez-García [b], Joanna Bojarska [c], Marcin Kozanecki [d], Jacek Michal Rynkowski [c]

[a] Departamento de Física y Química, Facultad de Ciencias Exactas y Naturales, Grupo de Investigación en Procesos Reactivos Intensificados con Reacción y Materiales Avanzados–PRISMA, Universidad Nacional de Colombia, Sede Manizales, Campus Palogrande, Cra 27 64–60, Apartado Aéreo 127, Manizales, Caldas, Colombia
[b] Departamento de Ingeniería Química, Facultad de Ingeniería y Arquitectura, Grupo de Investigación en Procesos Reactivos Intensificados con Reacción y Materiales Avanzados–PRISMA, Universidad Nacional de Colombia, Sede Manizales, Campus Palogrande, Cra 27 64–60, Apartado Aéreo 127, Manizales, Caldas, Colombia
[c] Institute of General and Ecological Chemistry, Lodz University of Technology, Zeromskiego 116, 90-924 Lodz, Poland
[d] Department of Molecular Physics, Lodz University of Technology, Zeromskiego 116, 90-924 Lodz, Poland

ARTICLE INFO

Article history:
Received 30 November 2014
Accepted after revision 24 February 2015
Available online 10 September 2015

Keywords:
Nanocrystalline zirconium oxide
Aqueous combustion
Thermodynamic modeling
Structural properties
Morphology

ABSTRACT

Nanocrystalline tetragonal zirconia powders have been synthesized by aqueous combustion using glycine (Gly) as a fuel and zirconyl nitrate (ZN) as an oxidizer. The effect of the fuel-to-oxidant molar ratio on the structural and morphological properties of nanocrystalline zirconia powders was studied. Thermodynamic modeling of the combustion reaction showed that the increase in the Gly:ZN molar ratio leads to the increase in theoretical combustion temperature, heat of combustion and amount of produced gases. Powder properties were correlated with the nature of combustion and results of thermodynamic modelling. The increase in the Gly:ZN molar ratio produces more agglomerated powders characterized by a lower degree of uniformity, a lower specific surface area and a slightly bigger crystallite size. On the other hand, the presence of hard agglomerates suppresses the volume expansion, stabilizing tetragonal zirconia, as confirmed by Rietveld refinement. The absence of cubic zirconia was confirmed by FTIR and Raman Spectroscopy. The increase in the calcination temperature led to more agglomerated, compact and less uniform powders. The nanocrystalline nature of zirconia is the reason for the formation of bigger crystallites, the increase in the relative amount of monoclinic phase and sample sintering after calcination at high temperature. The highest measured specific surface area of zirconia was 45.8 $m^2 \cdot g^{-1}$, obtained using a fuel-lean precursor.

1. Introduction

Nanocrystalline zirconium oxide (zirconia, ZrO_2) is one of the most important ceramic materials, shock- and corrosion-resistant, with wide variety of potential applications such as a structural and biomaterial, solid-state electrolyte, gas sensor and thermal barrier coating [1]. It also attracts a great attention as a catalyst or as a support

* Corresponding author at: Grupo de Investigación en Procesos Reactivos Intensificados con Reacción y Materiales Avanzados–PRISMA, Universidad Nacional de Colombia, Sede Manizales, Campus Palogrande, Cra 27 64–60, Apartado Aéreo 127, Manizales, Caldas, Colombia.
E-mail address: idobrosz-gomez@unal.edu.co (I. Dobrosz-Gómez).

http://dx.doi.org/10.1016/j.crci.2015.02.007
1631-0748/

for many reactions [2,3]. Moreover, the application of the nanosized metastable tetragonal zirconia particles, as a dispersed phase in ceramic materials, leads to the increase in their fracture toughness, strength and hardness [4]. Those unique properties of ZrO_2 have become a driving force for the development of alternative techniques for its preparation, among them the aqueous combustion synthesis [5]. It is a versatile, simple, safe, energy- and time-saving process, with capability to produce homogeneous, high purity and nanocrystalline ceramic powders [6]. The aqueous combustion synthesis involves the formation of a homogeneous oxidant-fuel precursor and its redox exothermic reaction, accompanied with a quick evolution of large volume of the gaseous products. The nature of the combustion and the properties of the resulting powder depend on the type and the amount of the fuel used in the process. According to Toniolo et al. [7], a good fuel should react non-violently, produce non-toxic gases and act as complexing agent to form metal cations. Glycine, one of the cheapest amino acids, is known to act as a complexing agent due to its carboxylic acid group at one end and amino group at the other. Such types of zwitterionic character of a glycine molecule can effectively complex metal ions of different ionic size, which helps in preventing their selective precipitation to maintain compositional homogeneity among the constituents. On the other hand, it can also serve as a fuel in the combustion reaction, being oxidized by nitrate ions [8]. Therefore, glycine was chosen as a fuel for the preparation of nanocrystalline zirconia powders in this study.

Several papers have already discussed the role of the fuel in controlling the morphology of the synthesized powders [7–11]. A zirconia nanosized single crystal has already been prepared by the combustion of an aqueous solution of metal nitrate and glycine [12]. Zirconia nanocrystalline powders were also synthesized using sucrose [13], glycine [9] and citric acid [14] as a fuel. However, in the most of these researches, the amount of the fuel and/or complexing agent has been fixed according to the concept of propellant chemistry [15]. Scarce systematic studies on the effect of the fuel-to-oxidant molar ratio on the nature of combustion and properties of zirconia nanocrystalline powders have been reported. As far as we know, the effect of calcination temperature on zirconia's properties [16,17], obtained by combustion method, has not also been presented. Moreover, in view of beneficial properties of metastable tetragonal zirconia particles, in the area of ceramic materials, we consider important to review its formation by different techniques: XRD, FTIR and Raman Spectroscopy. This is due to the fact that it is very difficult to distinguish between tetragonal and cubic phases of zirconia by a qualitative XRD analysis, as a result of both (400) and (004) lines splitting and (112) line broadening, as made by the most of researches.

Here, the combustion synthesis of nanocrystalline zirconia powders using glycine as a fuel and zirconyl nitrate as an oxidizer is reported. The study is focused on the effect of:

- the fuel-to-oxidant molar ratio on the properties (such as: specific surface area, crystalline structure, crystallite size, extent and nature of agglomerates) of nanocrystalline zirconia powders;
- sample morphology on tetragonal zirconia stabilization;
- calcination temperature on the microstructural evolution of zirconia powders.

For these purposes, the synthesized powders have been characterized by: TGA, specific surface area measurements, SEM-EDS, XRD, FTIR and Raman Spectroscopy. The thermodynamic modeling of the combustion reaction was carried out in order to study the role of the fuel-to-oxidant molar ratio on the heat of combustion, theoretical combustion temperature, number of moles of gases evolved in the reaction and the nature of combustion process. The results of thermodynamic modeling were correlated with powders properties.

2. Experimental

2.1. Synthesis

Zirconyl nitrate hydrate [$ZrO(NO_3)_2{\cdot}xH_2O$, Aldrich, purity 99%, ZN] and glycine [NH_2CH_2COOH, Mallinckrodt, purity 99.5%, Gly] were used as the starting materials. The different compositions of the redox mixtures (Gly:ZN) for the combustion were calculated using the total reducing (+9) and oxidizing (−10) valences of the starting materials: Gly and ZN, respectively. According to the principle of propellant chemistry [15], for stoichiometric redox reaction, the ratio of the net reducing valency of the fuel net to the oxidizing valency of the metal nitrate should be unity (maximum quantity of energy released in the combustion process). Therefore, the Gly:ZN molar ratio for the stoichiometric combustion should be 1.11. Moreover, fuel-lean (0.5 and 0.75) and fuel-rich (2) Gly:ZN precursors were applied for sample preparation. The studied range of the Gly:ZN molar ratio was chosen experimentally to guarantee the auto-ignition of the combustion process, considering that it takes place only in a limited range of the fuel-to-oxidant molar ratio (above and below the stoichiometric one). The amounts of fuel as well as of oxidant were taken to obtain approximately 3 g of the final product. The required amounts of starting materials were dissolved in the minimum amount of deionized water and mixed to obtain transparent aqueous solution of oxidant-fuel precursor. After its thermal dehydration at ca. 80 °C, as soon as a viscous liquid was formed, the temperature was increased up to ca. 250 °C. It led to the auto-ignited, fast, self-sustaining, flameless and non-explosive combustion of the liquid, accompanied with a rapid evolution of large amount of gases and formation of an amorphous powder (as confirmed by XRD, not shown here), indicating the incomplete combustion. The nature of the ignition and the aspect of the obtained powders depended on the fuel-to-oxidant molar ratio. Henceforth, these samples are indicated as raw powders. Subsequently, they were calcined in air, at 600 °C, with a ramp rate 3 °C·min^{-1}, for 4 hours at atmospheric conditions, in order to remove traces of unreacted starting materials (if any) and/or products of their decomposition and obtain pure and well-crystallized

zirconia oxides. Moreover, some representative samples were calcined at 800 and 1000 °C with the purpose of studying the effect of calcination temperature on their physicochemical properties. Before calcination, the raw powders were hand ground in an agate mortar. For all Gly:ZN molar ratios, a similar quantity of ZrO_2 powder after calcination process was obtained. An average efficiency of 75% of yield was achieved.

2.2. Characterization methods

The standard enthalpy of combustion (ΔH^0) and theoretical adiabatic flame temperature (combustion temperature) (T), as a function of the Gly:ZN molar ratio, were calculated using the following thermodynamic expressions:

$$\Delta H^0 = \left(\sum n\Delta H_f^0\right)_p - \left(\sum n\Delta H_f^0\right)_r \quad (1)$$

$$T = T_0 + \frac{(\Delta H_f^0)_p - (\Delta H_f^0)_r}{\Delta C_p} \quad (2)$$

where: n is number of the mol, $(\Delta H_f^0)_r$ and $(\Delta H_f^0)_p$ represent the enthalpies of formation of the reactants and products at 25 °C, respectively, T is theoretical adiabatic flame temperature, T_0 is the reference temperature (25 °C) and ΔC_p is the overall change in the heat capacity per mol. Table 1 contains the relevant thermodynamic data for various reactants and products.

The thermal stability of raw zirconia powders was characterized by thermogravimetric analysis (TGA), using a Setsys 16/18 thermogravimetric analyzer (Setaram). The crucible containing about 10 mg of sample was heated from room temperature (r.t.) to 800 °C in air, with a ramp rate of 3 °C·min^{-1}.

The morphology of ZrO_2 powders was studied using a scanning electron microscopy–energy dispersive spectroscopy (SEM-EDS) technique. SEM measurements were performed by JSM-5910LV microscope (JEOL, Japan), using an acceleration voltage of 15 kV, equipped with energy dispersive spectrometer (EDS) (Thermo Noran, USA). Images were recorded at several magnifications. The elemental analysis in the studied microarea of the oxide surface layer was determined by the EDS method, basing on the obtained characteristic X-ray spectra. The examined samples were placed in a holder and before analyzing were coated with a carbon monolayer, using Cressington 208 HR system (Cressington Scientific Instruments Ltd., UK), in order to reduce the charge build-up on the samples.

The crystalline structure identification and crystallite size determination of ZrO_2 powders was carried out using X-ray diffraction (XRD). Approximately 300 mg of sample, which had been hand ground in an agate mortar, was packed in the sample holder. XRD patterns were obtained at room temperature using a PANalytical's X'Pert-Pro MPD X-ray diffractometer (equipped with X'Celerator) with nickel-filtered Cu Kα radiation (λ = 1.5406 Å), operating at 40 kV and 30 mA. Divergent optics were used in a Bragg-Brentano (flat-plate sample) geometry, with the following slits: Soller (0.04 rad)–on incident and diffracted beams, fixed divergence (0.5°), antiscatter (1°). Data were collected in the 2θ range of 20–80°, with a step size of 0.0167° and step time of 10 s. Phase analysis was performed using X'Pert HighScore Plus software and JCPDS-ICDD PDF–2 database (International Centre for Diffraction Data-The Powder Diffraction File) in order to identify the crystalline phases. The quantitative phase analysis has been performed by the Rietveld refinement technique, via Hill and Howard's [20,21] procedure, using the following formula:

$$W_p = \frac{(Z \times S \times M \times V)_p}{\sum_i (Z \times S \times M \times V)_i} \quad (3)$$

where: W_p (wt. %) is the relative weight fraction of phase p in the mixture of i phases, S is the Rietveld scale factor, Z is the number of formula units in the unit cell, M is the molecular weight of the formula unit (atomic mass unit, u), V is the unit cell volume (Å^3) and i is an index running over all phases. The subscripts p and i are used for pth and ith phase. The tetragonal and monoclinic polymorphs of ZrO_2, with space group $P4_2/nmc$ and $P2_1/c$, respectively, were used as the starting models. The background in the XRD pattern was refined using a polynomial with five refinable coefficients. The peak shape was corrected using a pseudo-Voigt function.

The crystallite size (D_{XRD}) of ZrO_2 powders was determined by means of the X-ray line broadening method [22], according to the Scherrer equation (4).

$$D_{XRD} = \frac{k\ \lambda}{\beta\ \cos\theta} \quad \langle nm \rangle \quad (4)$$

where θ is the incidence angle for the hlk reflection (rad), β is the angular line width at medium height (rad), and k corresponds to the Scherrer constant (0.9).

The specific surface area was measured with Sorptomatic 1900 apparatus (Carlo Erba), at −196 °C, by determining the amount of nitrogen gas adsorbed as a

Table 1
Relevant thermodynamic data for various reactants and products [18,19].

Compound	ΔH_f^0 (kJ · mol^{-1})	C_p (J·mol^{-1}·K^{-1})
$ZrO(NO_3)_2H_2O_{(c)}$	−1820	–
$NH_2CH_2COOH_{(c)}$	−333	–
$ZrO_{2(c)}$	−1101.3	$69.668 + (7.53\cdot10^{-3}\cdot T) - (1.406\cdot10^{6}\cdot T^{-2})$
$CO_{2(g)}$	−393.8	$(19.8\cdot T) + (7.344\cdot10^{-2}\cdot T^2) - (5.602\cdot10^{-5}\cdot T^3) + (1.715\cdot10^{-8}\cdot T^4)$
$H_2O_{(g)}$	−242	$(32.24\cdot T) + (1.92\cdot10^{-3}\cdot T^2) + (1.055\cdot10^{-5}\cdot T^3) - (3.59\cdot10^{-9}\cdot T^4)$
$N_{2(g)}$	0	$(31.1\cdot T) - (1.357\cdot10^{-2}\cdot T^2) + (2.68\cdot10^{-5}\cdot T^3) - (1.168\cdot10^{-8}\cdot T^4)$
$O_{2(g)}$	0	$(28.11\cdot T) - (3.68\cdot10^{-6}\cdot T^2) + (1.746\cdot10^{-5}\cdot T^3) - (1.065\cdot10^{-8}\cdot T^4)$

(c): crystalline; (g): gas; T: absolute temperature (K); C_p: heat capacity at constant pressure; ΔH_f^0: enthalpy of formation at 25 °C.

Table 2
Stoichiometric coefficients of the combustion reaction (α–γ), standard enthalpy of combustion (ΔH^0), theoretical (T) and measured (T_m) adiabatic flame temperatures, as a function of the Gly:ZN molar ratio.

Gly:ZN molar ratio	α	β	χ	δ	ε	ϕ	φ	γ	Moles of gaseous product/Moles of ZrO_2	$-\Delta H^0$ (kJ·mol^{-1})	T (°C)	T_m (°C)
0.5	1	0.5	0	1	1	2.25	1.25	1.38	5.88	53.1	192	135
0.75	1	0.75	0	1	1.5	2.87	1.37	0.82	6.56	316.8	978	730
1.11	1	1.11	0	1	2.22	3.78	1.55	0	7.55	700.7	1725	1305
2	1	2	2	1	4	6	2	0	12	1642.5	2461	1210

T_m: maximum combustion temperature measured using a type-B thermocouple (Pt/Rh 70%/30%–Pt/Rh 94%/6% by weight).

monomolecular layer on the sample. Prior to the measurement, all samples were degassed for 4 h at 250 °C. The specific surface area, S_{BET} was calculated using BET equation [23]. Using the S_{BET} value, the geometrical mean particle size (D_{BET}) was calculated, assuming the presence of spherical particles, according to the following expression:

$$D_{BET} = \frac{6 \cdot 10^3}{\rho \; S_{BET}} \quad \langle nm \rangle \tag{5}$$

where: ρ (g·cm^{-3}) is theoretical density (6.12 g·cm^{-3}), and S_{BET} (m^2·g^{-1}) is the measured surface area of the ZrO_2 powder.

Fourier-transform infrared (FTIR) spectra of ZrO_2 powders were recorded by a Nicolet 6700 FT-IR spectrometer (Thermo Scientific, USA) with MCT detector (photoconductive detector HgCdTe), in the region of 4000–400 cm^{-1}, at room temperature, using the KBr (5 wt.%) pellet technique for functional group analysis.

Raman spectra were obtained using FT-Raman spectrometer MultiRAM (Bruker, Germany) with a YAG laser source of wavelength 1064 nm, laser power of 500 mW, and the spectrum resolution of 1 cm^{-1}.

3. Results and discussion

3.1. Thermodynamic modeling

The majority of solution combustion reactions are known as exothermic enough to provide high reaction temperatures, which are adequate for the combustion wave propagation and can also lead to the explosion if not appropriately controlled. In the present work, the combustion of glycine (Gly) – zirconyl nitrate hydrate (ZN) redox mixture was auto-ignited, self-propagated, flameless and non-explosive exothermic process for all studied Gly:ZN molar ratios. This reaction can be represented as follows:

$$\alpha ZrO(NO_3)H_2O_{(aq)} + \beta C_2H_5O_2N_{(aq)} + \chi O_{2(aq)} \rightarrow \delta ZrO_2(s) + \varepsilon CO_{2(g)} + \phi H_2O_{(g)} + \varphi N_{2(g)} + \gamma O_{2(g)}$$

where α to γ (Greek symbols) correspond to the stoichiometric coefficients of its reactants and products, as a function of the Gly:ZN molar ratio (Table 2).

One can see that the increase in the Gly:ZN molar ratio, leads to the increase in the amount of gaseous products (ε–γ), which could be an important factor controlling the specific surface area of the obtained ZrO_2. Moreover, if the amount of oxygen in the Gly:ZN mixture is in excess of that required for the complete combustion of the fuel (fuel-lean mixture), a portion of oxygen does not react and appears in the exhausts (γ), as previously reported in the case of glycine-cerium nitrate [8] and glycine-aluminum nitrate [7] combustion reactions. On the other hand, in the case of the oxygen shortage in the Gly:ZN mixture (fuel-rich mixture), the extra amount of atmospheric oxygen (χ) for the complete combustion of the fuel is needed.

Fig. 1 presents the heat of combustion ($-\Delta H^0$) and theoretical combustion temperature (T, theoretical adiabatic flame temperature), as a function of the Gly:ZN molar ratio, which were calculated by Matlab® using the relevant thermodynamic data (Table 1) for various reactants and products.

For Gly:ZN combustion reaction, the heat of combustion and theoretical combustion temperature significantly increase with an increase in the amount of fuel used for the combustion (Gly:ZN molar ratio). For both stoichiometric and fuel-rich Gly:ZN mixtures, the theoretical adiabatic flame temperature is significantly higher than 1170 °C, the temperature above which tetragonal ZrO_2 is stable, suggesting the effect of this parameter on the structural properties of ZrO_2. However, it should be emphasized that the measured combustion temperatures (T_m) were much lower than the calculated one, especially in the case of the sample prepared using fuel-rich Gly:ZN mixture, probably due to incomplete combustion reaction, radiative losses, and heating of air (Table 2). It should be also noted that these measurements can be characterized with some inaccuracy due to the very spontaneous character of the

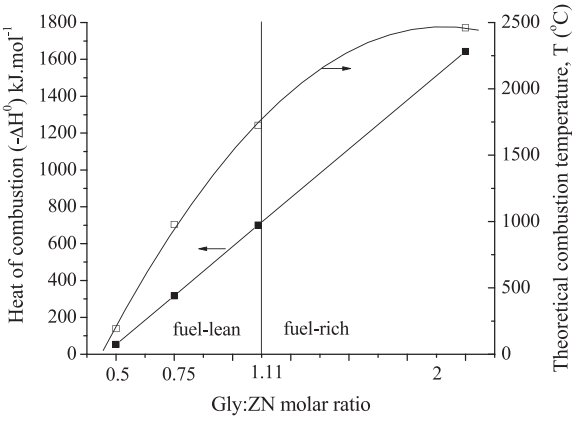

Fig. 1. Variation of heat of combustion (■) and theoretical combustion temperature (□) as a function of the Gly:ZNmolar ratio.

combustion process as well as thermocouple inertia and its punctual form of temperature measuring. The theoretical combustion temperature of Gly:$ZrO(NO_3)_2{\cdot}H_2O$ stoichiometric mixture, calculated in this work (ca. 2270 °C), is much higher than those reported in the literature for $Ce(NO_3)_3{\cdot}6H_2O$:Gly (ca. 1740 °C) [8] and $Fe(NO_3)_3{\cdot}9H_2O$:Gly (ca. 1520 °C) stoichiometric mixtures [24]. One can see that this temperature decreases when increasing the amount of molecules of water attached to the metal precursor. It suggests that water remaining in the metal nitrate-glycine solution at the temperature of auto-ignition strongly influences the adiabatic flame temperature. More hydrated metal precursors probably can ignite at relatively lower temperatures than water-free systems. Moreover, considering that this residual liquid must be transformed to the vapor and finally be heated as other combustion products, lower values of the resulting (real) combustion temperatures can be expected.

3.2. Sample synthesis

The color of the as-synthesized powders was found to change, from brownish to blackish, with an increase in the Gly:ZN molar ratio used for the synthesis. It could be related to:

- the presence of carbonaceous residue arising from unreacted glycine, especially evident in the case of the sample prepared using fuel-rich mixture due to insufficient amount of oxidizer specimen ($ZrO(NO_3)_2{\cdot}H_2O$);
- and lower real temperature of combustion, comparing to theoretical one necessary for a complete reaction. As it was expected, after calcination all powders were white.

During the combustion of the fuel-lean mixtures, the amount of gaseous products was much higher than that of the fuel-rich one, leading to the formation of more voluminous and apparently highly porous powders. This observation is contrary to the expected one, made on the basis of the reaction stoichiometry (Table 2, number of moles of gaseous products/moles of ZrO_2). We believe that the reason for this contradiction is related to much lower real temperature of combustion, comparing to the theoretical one necessary for a complete reaction, especially evident for the sample prepared by fuel-rich mixture. The change in the color of the released fumes, from dark yellow (reddish) to white, with an increase in the Gly:ZN molar ratio was also observed. This remark is in the discrepancy with the statement made by Reddy et al. [12] who reported that the color of the fumes during smoldering combustion changed from white-brown to brown with an increase in the Gly:ZN molar ratio. We believe that this inconsistency can be clarified as follows. According to the literature [7], self-sustaining nature of the combustion is a result of the following steps:

- the formation of the precursor mixture containing metal nitrate and glycine, used as combustible fuel;
- its dehydration which leads to nitrate decomposition giving oxides of nitrogen (NO_x) as a product;
- the reaction between the gaseous NO_x and the fuel generating heat and higher amount of gases;
- the homogeneous gas-phase, exothermic oxidation-reduction which increases the temperature of the intact viscous mixture at once adjoining the combustion zone;
- the quick reaction which is sustained until the entire intact zone will be consumed.

Considering those statements, we believe that the formation of NO_x can be the reason for the different colors of fumes released during the combustion realized using different ZN:Gly molar ratios. NO_x is a generic term for nitric oxide (NO, colorless gas) and nitrogen dioxide (NO_2, vivid orange gas). In the presence of air, the ratio between NO and NO_2 can change due to thermodynamic equilibrium, as proposed by Gómez-García et al. [25]. At lower temperatures (< 230 °C), the formation of NO_2 is favorable, at higher ones (> 630 °C) the formation of NO occurs. If a fuel-lean mixture was used for synthesis, a lower temperature for its complete combustion was required, leading to the formation of mostly NO_2 and related to it the reddish color of the fumes. In the case of synthesis using fuel-rich mixture, higher temperature for its complete combustion was necessary, leading to the formation of mostly colorless NO and related to it change in the color of the fumes to white.

3.3. Sample characterization

Fig. 2 presents the TG-DTG curves, in a stream of air, of raw powders synthesized using different Gly:ZN molar ratio. The TG thermograms of fuel-lean and stoichiometric samples exhibit two main regions of weight loss. The first one (ca. 3–17%, depending on the Gly:ZN molar ratio), continous and in general mayor, in the temperature range of 15–500 °C, with maximum at at ca. 330 °C, relates to the main decomposition and/or combustion of the raw powders, resulting in the formation of zirconium oxide. The second one, subsidiary (ca. 5%) takes place in the temperature range of 500–620 °C, presumably due to the oxidation of some carbonaceous residues to CO_2. One can see a slight shift of the maximum of the DTG curve, related to the carbonaceous residues oxidation, to the higher temperatures with an increase in the Gly:ZN molar ratio. For fuel-rich powder four main regions of weight loss are observed. The first one (ca. 30%), continuous in the temperature range of 15–260 °C, with the maximum at ca. 200 °C, relates to the unreacted glycine decomposition; the second one (ca.16%) in the temperature range of 260–320 °C, with the maximum at ca. 290 °C, and the third one (ca. 20%) in the temperature range of 320–500 °C, with the maximum at ca. 360 °C, can represent the main decomposition and/or combustion of the raw powders, resulting in the formation of zirconium oxide. The fourth one (ca. 2%) in the temperature range of 320–620 °C, with the maximum at ca. 565 °C, probably takes place due to the oxidation of some carbonaceous residues to CO_2. The total weight loss of the studied samples increases with an increasing amount of the glycine in the combustion mixture, according to the Gly:ZN molar ratio: 1:0.5 < 1:0.75 < 1:1.11 < 1:2. Moreover, one can see that in the case of

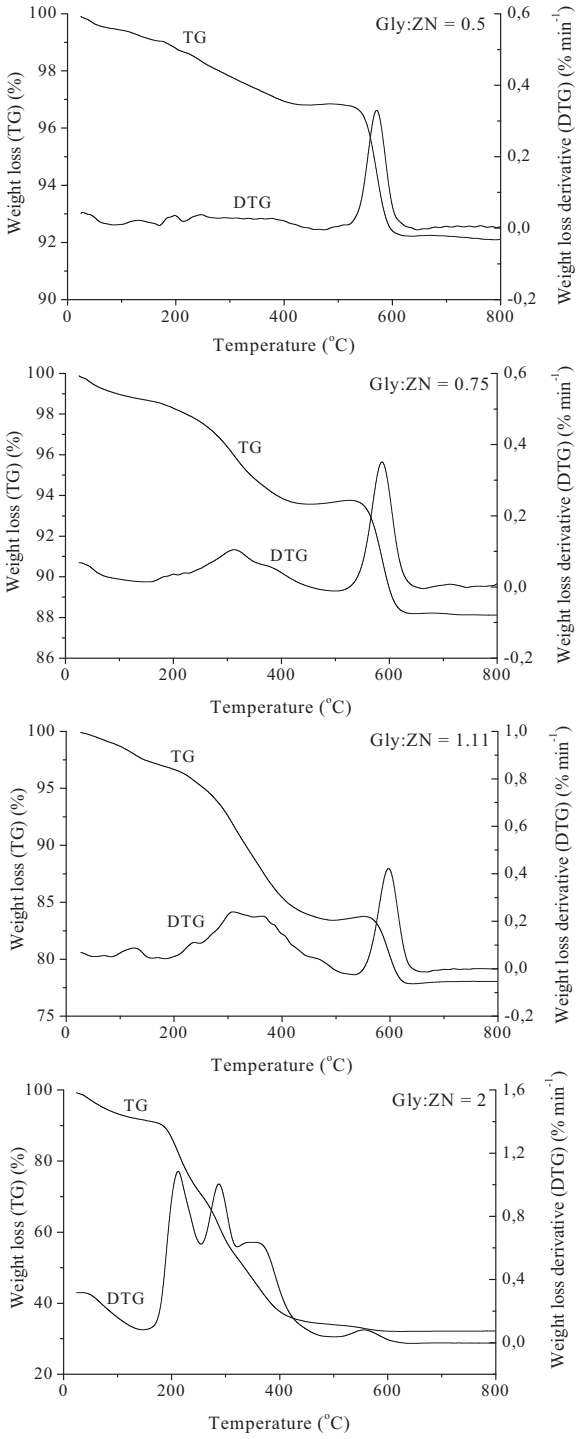

Fig. 2. TG-DTG curves depicting thermal decomposition of raw ZrO_2 powders in the air.

the fuel-rich sample (the darkest one) the weight loss related to the carbonaceous residues oxidation was the lowest one and took place at lower temperature than in the case of the rest of the studied powders. We consider that the un-reacted glycine decomposition took place at much lower temperature (ca. 200 °C), hence lower amount of carbonaceous residue was present in the sample. One can see that independently of the Gly:ZN molar ratio, at temperature above 600 °C, all raw ZrO_2 powders presented constant weight. We believe that thermal treatment at 600 °C is going to ensure their total decomposition, therefore, it was chosen as calcination temperature for further investigation.

Fig. 3a presents typical SEM micrographs of ZrO_2 obtained using different Gly:ZN molar ratios, calcined at 600 °C. The results show that all powders are uniform, voluminous and spongy in nature. They exhibited foamy and agglomerated particles with a wide distribution, strongly dependent on the Gly:ZN molar ratio. One can see that the registered agglomeration tendency increases as the Gly:ZN molar ratio increases. The samples prepared using Gly:ZN molar ratios ≤ 1.11 are loosely agglomerated and present a high amount of characteristic voids with typical sizes of 0.5–5 μm. The formation of these features can be attributed to the fast evolution of large amount of gases during the combustion process. Quick gaseous products formation disperses the heat of combustion, limiting the rise of temperature and reducing the possibility of premature, partial and local sintering of primary particles. Their size increases with an increase in the Gly:ZN molar ratio due to the increasing number of moles of gaseous products during the synthesis process (Table 2), with the maximum observed for stoichiometric Gly:ZN mixture. The powder prepared using excess of Gly presents lower degree of uniformity. It consists of mostly spherical particles with typical sizes of 1–5 μm, much bigger than those obtained using fuel-lean and stoichiometric Gly:ZN mixtures. Moreover, lower quantity of characteristic voids in its structure is observed probably due to the lower amount of gaseous products evolved during the combustion as well as high adiabatic flame temperature, as we mentioned above. For all samples, the EDS analysis showed the presence of zirconia and confirmed low concentration of impurities after calcination at 600 °C. On further increase in calcination temperature, more agglomerated and compact powders are formed (Fig. 3b). Moreover, the amount and the size of characteristic voids observed for the sample calcined at 600 °C decreases gradually. The uniform, voluminous and spongy nature of the samples is reduced after calcination at high temperature.

X-ray diffraction patterns of ZrO_2 powders, synthesized using different Gly:ZN molar ratio, calcined at 600 °C are presented in Fig. 4a.

Crystalline phases were identified by a comparison with the corresponding JCPDS files. XRD patterns of all ZrO_2 powders, calcined at 600 °C correspond to both monoclinic (JCPDS card no.: 00-037-1484) and tetragonal (JCPDS card no.: 00-050-1089) structures. For all samples, the tetragonal phase is a principal one (Table 3).

It should be noticed that both tetragonal and cubic phases produce a broad diffraction peak at $2\theta = 30°$, making differentiation between them difficult, especially if the sample is characterized with small particle size and/or poor crystallinity. Therefore, the XRD studies were complemented with FTIR and Raman experiments. One can

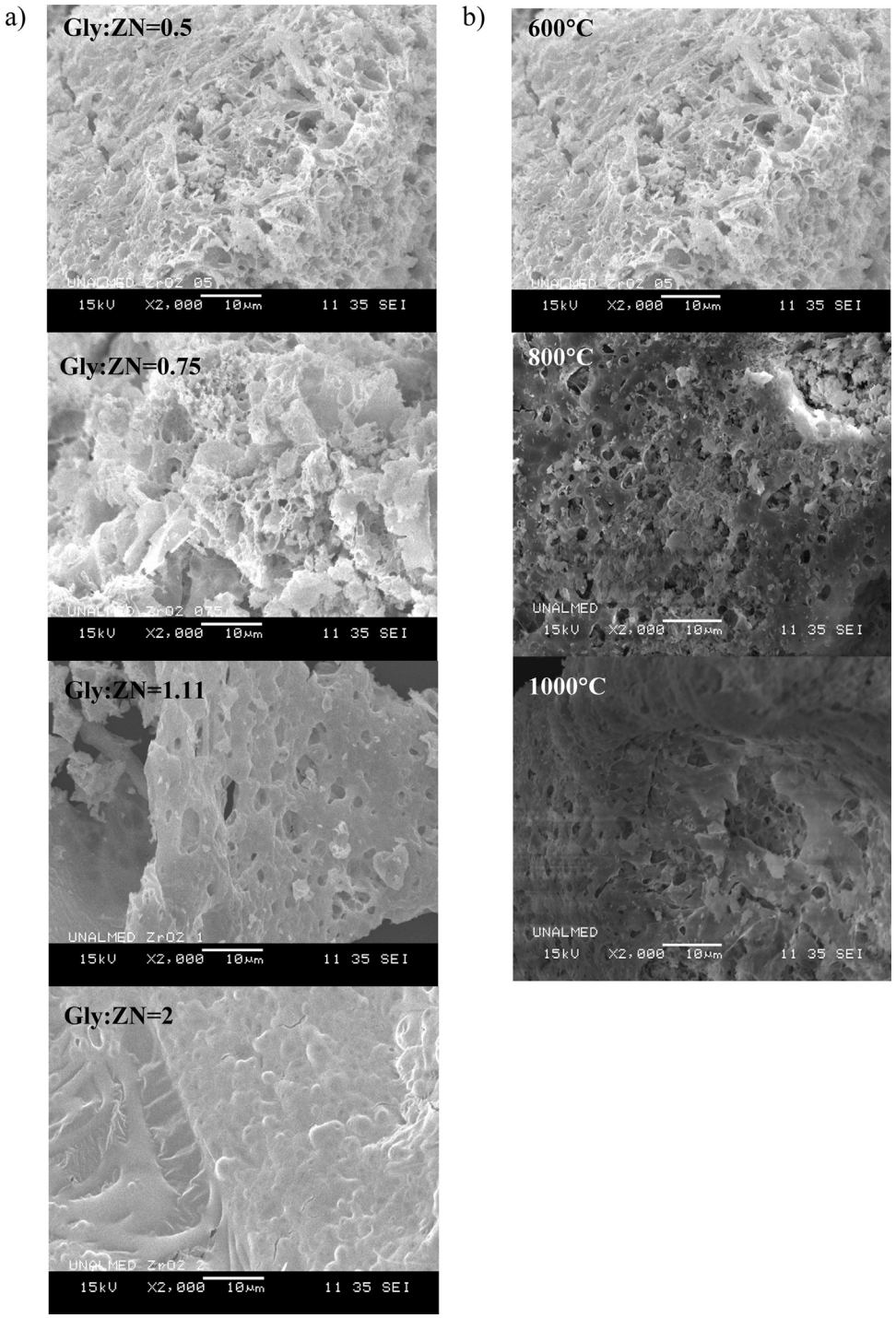

Fig. 3. Secondary electron (SE) photomicrographs of ZrO_2 powders prepared using: a: different Gly:ZN molar ratios, calcined at 600 °C; b: Gly:ZN = 0.5, calcined at different temperatures. Magnifications: × 2000.

see a very slight increase in the relative amount of tetragonal phase with an increase in the Gly:ZN molar ratio (Table 3). Considering that the agglomeration tendency of synthesized powders was also increasing with an increase in the Gly:ZN molar ratio (Fig. 3a), it could be suggested that the presence of hard aggregates promotes the formation of metastable-tetragonal nanocrystalline zirconia, as previously proposed by Skukla et al. [26]. The mechanism of t-zirconia stabilization can be based on the volume expansion associated with the tetragonal to

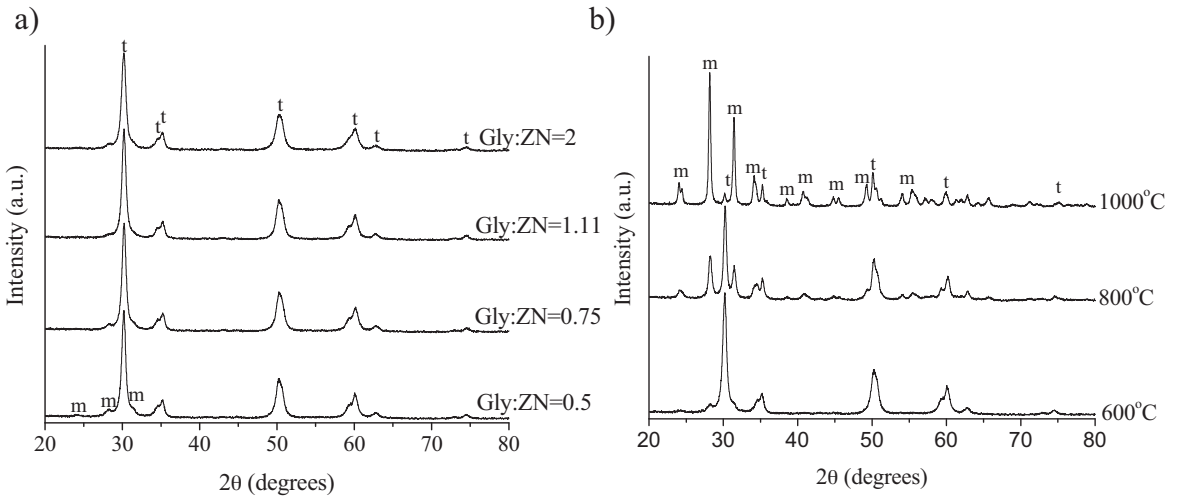

Fig. 4. X-ray diffraction of ZrO_2 powders prepared using: a: different Gly:ZN molar ratios, calcined at 600 °C; b: Gly:ZN = 0.5, calcined at different temperatures; the peak marked as *m* and *t* corresponds to monoclinic (JCPDS No. 00-037-1484) and tetragonal (JCPDS No. 00-050-1089) structures, respectively.

Table 3
Characterization of ZrO_2 powders prepared using different Gly:ZN molar ratios, calcined at 600 °C.

Gly:ZN molar ratio	Relative amount of crystalline phases (%)		D_{XRD} (nm)		S_{BET} ($m^2 \cdot g^{-1}$)	V_p ($cm^3 \cdot g^{-1}$)	D_p (nm)	D_{BET} (nm)	ψ
	T	M	T	M				T	T
0.5	95.5	4.5	13.4	11.7	45.8	0.190	13.4	21.4	1.60
0.75	96.1	3.9	14.9	11.7	40.7	0.180	14.1	24.3	1.62
1.11	96.1	3.9	15.0	11.7	40.2	0.198	14.0	24.4	1.63
2	96.8	3.2	15.5	11.1	23.3	0.054	6.5	42.1	2.72

D_{XRD}: crystallite size calculated basing on XRD line broadening; T: tetragonal phase; M: monoclinic phase; S_{BET}: specific surface area determined by the BET method; V_p: pore volume taken at $p/p_0 = 0.99$; D_p: average pore diameter determined by the BJH method; D_{BET}: particle size calculated for tetragonal zirconia, based on the specific surface area; $\psi = (D_{BET}/D_{XRD})$.

monoclinic ZrO_2 transformation. The presence of hard agglomerates suppresses the volume expansion, stabilizing the tetragonal zirconia. The primary crystallite size of powders calcined at 600 °C, determined using the Scherrer equation (D_{XRD}), is presented in Table 3. The slight increase in the crystallite size with the increase in the Gly:ZN molar ratio can be attributed to an increase in flame temperature, which assists crystal growth. There is also a correlation between the increase in the crystallite size and the reduction in the specific surface area, as a function of increasing fuel content (Table 3). As similar observation has already been done by Toniolo et al. [7] in the case of alumina synthesis by the glycine-nitrate combustion. The zirconia powders obtained using fuel-lean mixture present the highest specific surface area, whose value decreases as the Gly:ZN molar ratio increases. We believe that the observed tendency is directly related to the nature of combustion process. The application of Gly shortage results in the low reaction enthalpy (Table 2), remaining low local temperature of formed particles and preventing their agglomeration. Moreover, this reaction was accompanied with the evolution of large amount of gaseous products (see Sample synthesis section) leading to the formation of more porous structure (Table 3). As the Gly:ZN molar ratio increases, higher combustion temperatures are generated (Table 2) and lower amount of gases are evolved (see Sample synthesis section), leading to the formation of a dense structure (Table 3). It should be also noted that the difference between the surface area of the powders synthesized by the fuel-lean and stoichiometric mixtures is not as significant as in the case of that between the fuel-lean and fuel-rich ones. This may be attributed to the very significant difference in the corresponding flame temperatures (Table 2), as also previously observed by Purohit et al. [8] for cerium nitrate-glycine combustion. As far as we know, the surface area of 45.8 $m^2 \cdot g^{-1}$, obtained in this study using stoichiometric Gly:ZN mixture, is the highest one reported in the literature for ZrO_2 prepared by combustion method.

Fig. 5 shows the representative N_2 adsorption–desorption isotherm of ZrO_2 prepared using a molar ratio Gly:ZN = 0.5. All four analysed samples showed type IV isotherms, according to the IUPAC clasification, with hysteresis loops (type A, according to de Boer, or H1) typical of mesoporous materials. The hysteresis loop is associated with the capillary condensation taking place in

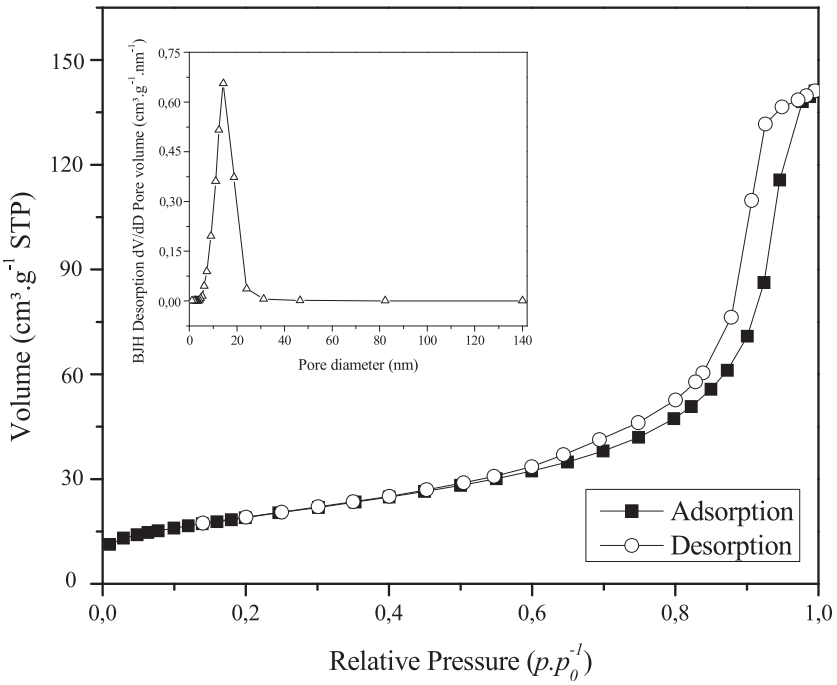

Fig. 5. The representative N_2 physisorption isotherm and BJH pore size distribution of ZrO_2 prepared using a molar ratio Gly:ZN = 0.5.

the mesopores signifying the preservation of the mesoporous structure even after calcination at elevated temperature. The type A hysteresis loop is attributed to the cylindrical shaped pores. A typical pore size distribution for this sample is included in Fig. 5. The sample exhibits a uninodal pore size distribution.

Table 3 presents additionally the geometrical particle size (D_{BET}) of ZrO_2 powders calcined at 600 °C, estimated from BET data assuming that the particles are spherical. For all samples, the calculated D_{BET} values are higher than those of the D_{XRD}. This deviation can be explained by a potential presence of small agglomerates and grain boundary interfaces in ZrO_2 powders, which are not available to N_2 gas during the BET analysis. Moreover, the XRD technique can detect the subgrains within particles. The ψ ($\psi = D_{BET}/D_{XRD}$) factor, which reflects the extent of agglomeration of the primary crystallites, was also estimated (Table 3). The ψ value increases from ca. 1.6 for fuel-lean synthesized zirconia to 2.72 for fuel-rich one, indicating that the extent of agglomeration increases as a function of the increasing amount of the fuel used for combustion.

Fig. 4b shows the XRD patterns of one of zirconia powders (Gly:ZN = 0.5) calcined at different temperatures. On the further increase in calcination temperature, the narrowing of main diffraction peaks, in comparison to the sample calcined at 600 °C, is registered due to the formation of bigger crystallites (Table 4). Moreover, the amount of the monoclinic phase increases, probably due to the observed crystal growth. After calcination at 800 °C, almost 50% of tetragonal phase is transformed into a monoclinic one (Fig. 4b, Table 4). After calcination at 1000 °C, zirconia presents mainly monoclinic phase (98.5%). Its crystallite size is ca. 32 nm. Upon an increasing calcination temperature, a significant decrease in the surface area of ZrO_2 (ca. 70%) as well as an increase in the powders crystallite size is observed (Table 4). For samples calcined at 800 and 1000 °C, the calculated D_{BET} values are significantly higher than those of the D_{XRD} due to the increasing amount of agglomerates (Fig. 3b). The ψ value

Table 4
Characterization of ZrO_2 powders prepared using Gly:ZN = 0.5, calcined at different temperatures.

Calcination temperature (°C)	Relative amount of crystalline phases (%)		D_{XRD} (nm)		S_{BET} ($m^2 \cdot g^{-1}$)	V_p ($cm^3 \cdot g^{-1}$)	D_p (nm)	D_{BET} (nm)	ψ
	T	M	T	M				T	T
600	95.5	4.5	13.4	11.7	45.8	0.190	13.4	21.4	1.60
800	55.5	44.5	18.1	17.5	26.5	0.058	6.8	37.0	2.04
1000	1.5	98.5	33.7	31.7	12.6	0.015	2.5	81.1	2.56

D_{XRD}: crystallite size calculated basing on XRD line broadening; T: tetragonal phase; M: monoclinic phase; S_{BET}: specific surface area determined by the BET method; V_p: pore volume taken at $p/p_0 = 0.99$; D_p: average pore diameter determined by BJH method; D_{BET}: particle size calculated for tetragonal zirconia, basing on the specific surface area; $\psi = (D_{BET}/D_{XRD})$.

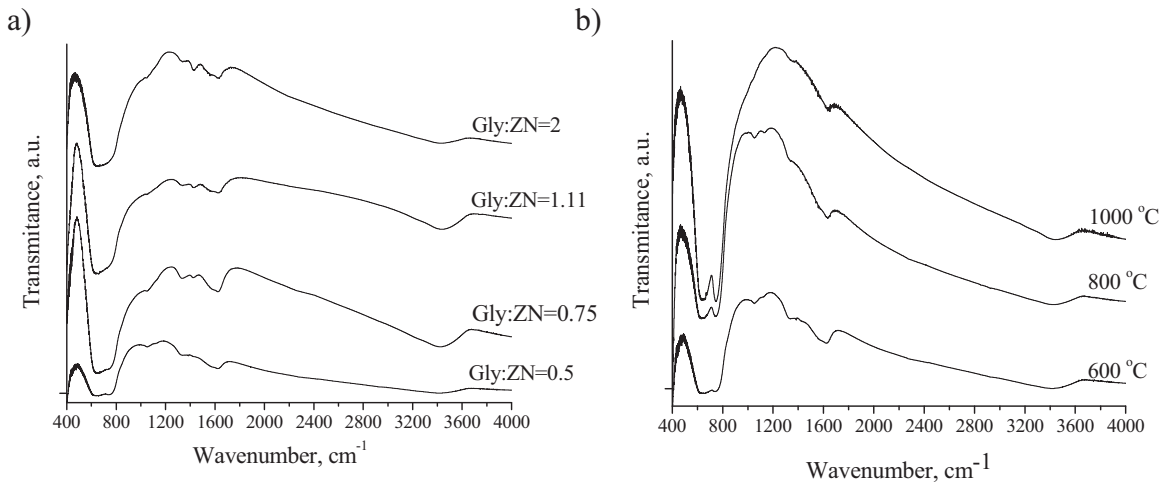

Fig. 6. FT-IR spectra of the ZrO_2 powders prepared using: a: different Gly:ZN molar ratio, calcined at 600 °C; b: Gly:ZN = 0.5 molar ratio, calcined at different temperatures.

increases by 40% with an increase in calcination temperature, confirming the extent of agglomeration.

In tetragonal zirconia, the smallest Bravais cell contains four oxygen ions and the tetrahedral surrounding oxygen are deformed (i.e. they are expanded along the *z*-axis). Therefore, each movement of oxygen atoms undergoes threefold splitting. Finally, the movements of the four oxygen atoms combine giving rise to four nondegenerate modes and to four doubly degenerate ones. Four of them are IR active and four Raman active. As a result of the combining movements of oxygens with the movements of zirconium ions and subtracting the acoustical modes, three IR bands (475, 580 and 670 cm^{-1}, each of them undergoing TO-LO splitting) and six Raman bands (145, 265, 313, 460, 600, 645 cm^{-1}) for the spectrum of tetragonal zirconia should be observed [27].

The FTIR spectra of the samples prepared using different Gly:ZN molar ratios, calcined at 600 °C are presented in Fig. 6a. The stretching frequencies of Zr–O vibrations can be observed in the 400–1190 cm^{-1} frequency region. For samples calcined at 600 °C (Fig. 6a), the FTIR spectra display an intense absorption with a maximum at 475 cm^{-1} characteristic of tetragonal zirconia. These spectra are quite similar to those observed and described previously (see Fig. 2 in Ref. [28] and Fig. 3 in Ref. [27]). The presence of monoclinic phase is not evident since no additional bands are detected, in particular at 510 and 740 cm^{-1} (Fig. 6a).

However, under increasing calcination temperature the band at 740 cm^{-1} becomes visible (Fig. 6b), which intensity increases with an increase in calcination temperature, confirming the presence of monoclinic phase in these powders. In addition, the bands at 1055, 1330 and 1430 cm^{-1} are probably due to the presence of carbonate species, which are variable with respect to calcination temperature and crystalline structure of the oxides (Fig. 6b). The presence of a broad band in the region of 3000–3600 cm^{-1} is attributed to the O–H stretching of physically adsorbed water. Our observations are similar to those presented in the literature [13,29].

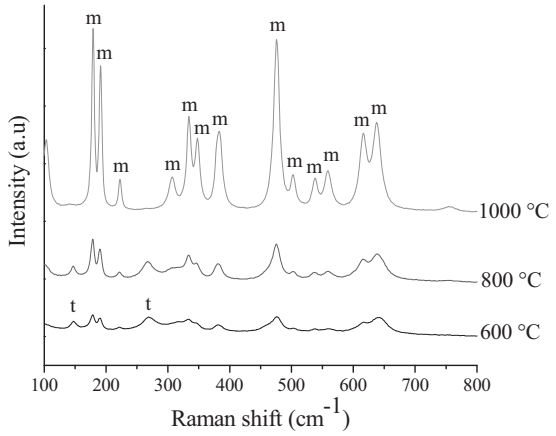

Fig. 7. Raman spectra of the ZrO_2 powders prepared using Gly:ZN = 0.5, calcined at different temperatures.

In order to study zirconia phase transformation and to confirm the phases present in the studied powders, Raman spectroscopy analysis was also performed with one of studied samples, calcined at different temperatures (Fig. 7). The bands at 174, 184, 215, 303, 330, 345, 380, 474, 499, 537, 559, 617 and 638 cm^{-1} are typical of the monoclinic phase of zirconia and those at 145, 265, 313, 460, 600, 645 cm^{-1} are representative of the tetragonal one. The Raman spectrum for the sample calcined at 600 °C is of a low intensity. However, the characteristic lines for both ZrO_2 structures were identified in the Raman spectrum collected for the sample calcined at 600 °C.

The presence of a doublet at 170–185 cm^{-1}, characteristic of the monoclinic zirconia phase, was registered after calcination even at 600 °C confirming that this is a sufficient temperature for the initiation of monoclinic ZrO_2 formation. The band at 303 cm^{-1} may overlap with tetragonal and monoclinic phases [13]. The most of the

Table 5
Comparison of some representative textural and morphological properties of ZrO_2 powders prepared using different methods and calcined at different temperatures.

Preparation method	Calcination temperature (°C)	Relative amount of T (%)	D_{XRD} (nm)	Specific surface area ($m^2 \cdot g^{-1}$)	Reference
Precipitation	500	5	n.r.	38.3	[31]
Precipitation/digestion	500	30	n.r.	75.7	[31]
Precipitation	500	n.r.	9.5	74.0	[32]
Precipitation	900	n.r.	24.9	16.0	[32]
Commercial ZrO_2	500	0	500	35	[33]
Polymerized organometallic compound	700	30	20	8	[33]
Precipitation	600	n.r.	10.5	n.r.	[27]
Precipitation	900	n.r.	13	n.r.	[27]
Sol-gel like	550	n.r.	19	4.5	[34]
Combustion (sucrose as the fuel; O/F = 0.2)	600	92	n.r.	31.1	[13]
Combustion (sucrose as the fuel; O/F = 0.2)	1100	0	n.r.	n.r.	[13]
Combustion (citric acid as the fuel; O/F = 0.67)	600	93	9	n.r.	[14]
Combustion (Gly:ZN = 1.11)	400	n.r.	20	17	[9]
Combustion (Gly:ZN = 0.5)	600	95.5	13.4	45.8	This study
Combustion (Gly:ZN = 0.5)	1000	1.5	33.7	12.6	This study

D_{XRD}: crystallite size calculated based on XRD line broadening; T: tetragonal phase.

tetragonal phase is transformed to the monoclinic one at a temperature of 1000 °C. This is proved by the lack of bands at 145 and 265 cm^{-1} assigned to tetragonal ZrO_2. Moreover, the absence of the bands at 150, 250, 360, 480 and 625 cm^{-1} confirms that no cubic phase is present in all studied powders. The overall half-width at half-height of the bands of Raman spectrum is proportional to the inverse of the grain size [13]. The broad bands in the studied spectra indicate the presence of particles in the nanoregime. The present results agree with those obtained by XRD. Quantitative phase analysis of the obtained ZrO_2 spectra (Fig. 7), estimated as proposed by Kim et al. [30], shows that the powder calcined at 600 °C is at 72.8% monoclinic, calcined at 800 °C in 82.6% and that at 1000 °C in 97.9%. One can see that these results are in disagreement with the quantitative phase analysis made basing on the XRD patterns (Table 3). We believe that it can be interpreted in the terms of:

- phase transformation of ZrO_2 which starts from the surface region, progressing to the bulk; the initial change of the phase at the surface can be sensitively detected by Raman spectroscopy rather than XRD;
- the fact that monoclinic zirconia is a stronger scatter that tetragonal one; Raman spectroscopy is superior in discerning the monoclinic phase, particularly when the monoclinic fraction is small [30]. We have observed that the Raman peak ratio $I_m(184\,cm^{-1})/I_t(145\,cm^{-1})$ is ca. 8 times bigger than the XRD one $I_m(-111)/I_t(111)$.

Table 5 presents a brief comparison of some representative textural and morphological properties of ZrO_2 powders obtained in this study with those reported in the open literature, prepared using different preparation techniques and calcined at different temperatures. One can see that the specific surface area of ZrO_2 powders prepared by combustion method, using citric acid and sucrose as fuels, is definitively lower than that obtained in this study. Moreover, they are characterized with slightly lower amount of tetragonal phase, if reported. However, this analysis is especially difficult since, in most of the research papers, the presence of tetragonal zirconia was confirmed only on the basis of XRD data. Compared to other preparation methods, ZrO_2 obtained by combustion is characterized with both the highest percentage of tetragonal phase and the highest specific surface area value. Independently of the preparation method, its sintering at high temperature due to the phase transformation accompanied with an increase in crystallite size can be seen.

4. Conclusions

Nanocrystalline tetragonal zirconia powders have been successfully prepared by aqueous combustion synthesis using glycine as a fuel and zirconyl nitrate as an oxidizer. The results of thermodynamic modeling as well as physicochemical characterization were correlated with powder properties. The most significant results can be summarized as follows:

- Gly:ZN molar ratio vs. properties of zirconia: the increase in Gly:ZN molar ratio led to:
  - the increase in agglomeration tendency and decrease in degree of sample uniformity; this due to the lower amount of gaseous products evolved during combustion reaction as well as high adiabatic flame temperature,
  - the slight increase in the powders crystallite size due to the increase in flame temperature, which assists crystal growth,
  - the decrease in specific surface area; Gly shortage led to low reaction enthalpy and low local temperature of formed particles, preventing their agglomeration and creating more porous structure,
  - a fuel-lean ratio was found as favorable to produce specific zirconia properties,
  - the detailed studies performed by Rietveld analysis, FTIR and Raman Spectroscopy confirmed the predominant presence of metastable tetragonal zirconia;

- sample morphology vs. tetragonal zirconia stabilization: the presence of hard agglomerates (powder with Gly excess, high reaction enthalpy, high adiabatic flame temperature, low amount of evolved gases) suppresses the volume expansion, stabilizing the tetragonal zirconia;
- calcination temperature vs. microstructural evolution of zirconia: the increase in calcination temperature led to more agglomerated, compact and less uniform powders. The nanocrystalline nature of the zirconia is the reason for bigger crystallites formation, the increase in the relative amount of monoclinic phase and sample sintering after calcination at high temperature.

Acknowledgments

Colciencias-Universidad Nacional De Colombia, Sede Manizales is gratefully acknowledged for financial support (Convocatoria 613 de 2013). The authors are also grateful to M. Sc. Eng. Ana Catalina Duque Salazar for her help in performing some experimental studies.

References

[1] M.M. Rashad, H.M. Baioumy, J. Mater. Proc. Tech. 195 (2008) 178.
[2] M. Mokhtar, S.N. Basahel, T.T. Ali, J. Mater. Sci. 48 (2013) 2705.
[3] M. Kantcheva, C. Koz, J. Mater. Sci. 42 (2007) 6074.
[4] R.H.J. Hannink, P.M. Kelly, B.C.J. Muddle, J. Am. Ceram. Soc. 83 (2000) 461.
[5] G.D. Yadav, B.A. Gawade, Catal. Today 207 (2013) 145.
[6] S.T. Aruna, A.S. Mukasyan, Curr. Opin. Solid State Mater. Sci. 12 (2008) 44.
[7] J.C. Toniolo, M.D. Lima, A.S. Takimi, C.P. Bergmann, Mater. Res. Bull. 40 (2005) 561.
[8] R.D. Purohit, B.P. Sharma, K.T. Pillai, A.K. Tyagi, Mater. Res. Bull. 36 (2001) 2711.
[9] T. Mimani, K.C. Patil, Mater. Phys. Mech. 4 (2001) 134.
[10] F.A. Deorsola, D. Vallauri, J. Mater. Sci. 46 (2011) 781.
[11] T. Lu, Y. Pan, J. Mater. Sci. 45 (2010) 5923.
[12] B.S.B. Reddy, I. Mal, S. Tewari, K. Das, S. Das, Metal. Mater. Trans. A 38 (2007) 1786.
[13] K. Boobalan, R. Vijayaraghavan, K. Chidambaram, U. Mudali, K. Mudali, B. Raj, J. Am. Ceram. Soc. 93 (2010) 3651.
[14] R.D. Purohit, S. Saha, A.K. Tyagi, Mater. Sci. Eng. B 130 (2006) 57.
[15] S.R. Jain, K.C. Adiga, V.R. Pai Verneker, Combust. Flame 40 (1981) 71.
[16] A. Adamski, P. Jakubus, Z. Sojka, Mater. Sci. Poland 26 (2008) 374.
[17] A. Adamski, P. Jakubus, Z. Sojka, Nukleonika 51 (2006) 27.
[18] R.H. Perry, C.H. Chilton, Chemical Engineers Handbook, 7th Ed., McGraw-Hill, New York, 1997.
[19] J.A. Dean (Ed.), Lange's Handbook of Chemistry, 15th Ed., McGraw-Hill, New York, 1999.
[20] R.J. Hill, C.J. Howard, J. Appl. Crystallogr. 20 (1987) 467.
[21] H.M. Rietveld, J. Appl. Crystallogr. 2 (1969) 65.
[22] H. Klug, L. Alexander, X-ray diffraction procedures for polycrystalline and amorphous materials, John Wiley and Sons, New York, 1974, pp. 618–708.
[23] S. Brunauer, P.H. Emmett, E. Teller, J. Am. Chem. Soc. 60 (1938) 309.
[24] A.S. Mukasyan, P. Epstein, P. Dinka, Proc. Combust. Inst. 31 (2007) 1789.
[25] M.Á. Gómez-García, V. Pitchon, A. Kiennemann, Environ. Int. 31 (2005) 445.
[26] S. Skukla, S. Seal, R. Vij, S. Bandhopadhyay, Z. Rahman, Nano Lett. 2 (2002) 989.
[27] V. Sánchez Escribano, E. Fernandez López, M. Panizza, C. Resini, J.M. Gallardo Amores, G. Busca, Solid State Sci. 5 (2003) 1369 [and references therein].
[28] E. Fernandez López, V. Sánchez Escribano, M. Panizza, M.M. Carnasciali, G. Busca, J. Mater. Chem. 11 (2001) 1891.
[29] K. Pokrovski, K.T. Jung, A.T. Bell, Langmuir 17 (2001) 4297.
[30] B.K. Kim, J.W. Hahn, K.R. Han, J. Mater. Sci. Lett. 16 (1997) 669.
[31] S. Jaenicke, G.K. Chuah, V. Raju, Y.T. Nie, Catal. Surv. Asia 12 (2008) 153.
[32] H. Liu, L. Feng, X. Zhang, Q. Xue, J. Phys. Chem. 99 (1995) 332.
[33] T.G. Kuznetsova, V.A. Sadykov, Kin. Catal. 49 (2008) 886.
[34] I. Dobrosz-Gómez, I. Kocemba, J.M. Rynkowski, Appl. Catal. B Environ. 83 (2008) 240.